Civil Engineering Infrastructures Journal, 53(1): 137– 159, June 2020
Print ISSN: 2322-2093; Online ISSN: 2423-6691
DOI: 10.22059/ceij.2019.280596.1580

Investigation of the Effects of Link Beam Length on the RC Frame Retrofitted with the Linked Column Frame System

Ezoddin, A.R.[1*], Kheyroddin, A.[2] and Gholhaki, M.[3]

[1] Ph.D. Candidate, Civil Engineering Faculty, Semnan University, Semnan, Iran.
[2] Professor, Civil Engineering Faculty, Semnan University, Semnan, Iran.
[3] Associate Professor, Civil Engineering Faculty, Semnan University, Semnan, Iran.

Received: 05 May 2019; Revised: 23 Oct. 2019; Accepted: 23 Oct. 2019

ABSTRACT: This study investigates the effect of different link beam lengths in the Reinforced Concrete (RC) frame retrofitted with the Linked Column Frame (LCF) system. It also investigates the ratio of the link beam length (e) to the span length of the RC frame (L) from 0 to 1.5 for the 9 models of the RC frame retrofitted by the LCF system has been investigated. In addition, it studies the formation of plastic hinges in the RC and Linked Column (LC) frame, distribution of stiffness between the RC and LC frame and the ratio of the structural displacement with the formation of the first plastic hinge in the member of the RC frame at the collapse prevention level ($\Delta_{p\ LCF}$) to the structural displacement with the formation of the first plastic hinge in the link beam ($\Delta_{y\ LCF}$) has been studied. Based on the nonlinear static analysis results, the model with the ratio of e/L= 0.45 has a better performance than other different lengths of the link beam. In this model, the stiffness of the LC frame has increased about 78% in comparison with the model with the ratio of e/L that is more than 0.6. Also, the ratio of $\Delta_{p\ LCF}$ to $\Delta_{y\ LCF}$ for the model of e/L = 0.45 in comparison with two models of e/L = 0.3 and 0.6 is more about 14% and 22%, respectively. It means that, the model of e/L = 0.45 has more potential to reach the performance level of Rapid Repair (RR) to occupancy.

Keywords: Link Beam, Linked Column Frame System, Nonlinear Static, Plastic Hinge, Retrofitting.

INTRODUCTION

After the earthquake of Northridge and Kobe in 1991 and the observation of significant damage to structures in these earthquakes, the seismic design of the structures was fundamentally changed. ATC (Applied Technology Council, 1996) and FEMA (Building Seismic Safety Council, 2000) are one of the most important codes to improve existing structures. These codes divide the possible damages based on the importance of the building and its efficacy after the earthquake. Therefore, they have defined the levels of performance. The adequate solution for protecting the main structural members and reducing the destructive effects of earthquakes use of structural systems are combined with the replaceable fuse members, which due to the ductile behavior and seismic energy dissipation are next to the main members of the structure. Relatively low cost

* Corresponding author E-mail: aezoddin@semnan.ac.ir

and the easy repair process in these systems lead to the rapid return to occupancy after an earthquake.

Several methods are used to retrofit the reinforced concrete, such as the concrete jacket or steel jacket, Fiber Reinforced Polymers (FRP) (Kianmofrad et al., 2018; Haji et al., 2019), adding steel bracing (internal and external) (Kheyroddin et al., 2019a,b; Hemmati et al., 2020), adding concrete shear wall or Steel Plate Shear Walls (SPSWs) (Broujerdian et al., 2017), adding dampening and the new method retrofitting using the LCF system.

The idea behind the LCF system was used by Nader et al. (2000) as the wide bases of the Oakland river bridge in California. The linked beams at the base of this bridge designed in the earthquake has shear yielding behavior and after the failure the link beams can easily be replaced. The energy dissipation and ductility of these members will limit the inelastic deformation and reduce the failure in the moment frame system. The behavior of the linked beam in the LCF system is similar to the behavior of the linked beam in the frames with the Eccentric Braced Frame (EBF). Based on the length of the link beam, these members act in shear or flexural yielding.

Bouwkamp et al. (2016) introduced the concept of the vertical link (V-EBF) and they studied experimental and analytical model of the V-EBF system. The experimental results showed that ultimate shear strength of vertical link is more than two times of yielding strength. Fintel and Ghosh (1981) used the structural fuse concept for the beams of the Moment Resisting Frame (MRF) with the strong columns-weak beam. In some other cases, the members with the function of protecting the main structure were considered as the structural fuse (Shahrooz et al., 2017; Lu et al., 2018; Tong et al., 2018; Li et al., 2019). Zahrai and Ezoddin (2018) to improve the efficiency of the RC structures, proposed a new structural system to prevent progressive collapse in intermediate RC frame structures, called cap or hat truss. The analysis results showed that this system can reduce the average vertical displacement and column axial force transferred to adjacent columns about 56% and 61%, respectively due to sudden removal of the column. Today, the application of replaceable fuse members is very general because they are easily replaced and able to protect the main structural members and restrict their damage in them.

Buckling-Restrained Braces (BRB) (Abdollahzadeh and Banihashemi, 2013; Bai and Ou, 2016; Pandikkadavath and Sahoo, 2017; Xu et al., 2018; Wang et al., 2019), Added Damping and Stiffness (ADAS) and Triangular-Plate Added Damping and Stiffness (TADAS) (Tsai et al., 1993; Dargush and Soong, 1995; Tena-Colunga, 1997; TahamouliRoudsari et al., 2018), Steel Shear Panels (Xu et al., 2016; Lin et al., 2019), and dissipative connection in concentric braced frame (Mohsenzadeh and Wiebe, 2018) are among the systems with replaceable fuse members.

The LCF structural system consists of two parts: one of the main lateral load bearing system of the structure which is a LC frame, and secondary lateral load system which includes a MRF. In the LC frame system, the replaceable link beams provide the initial stiffness of the system and then energy dissipation due to yielding and cause the displacement and ductility in the building to be increased (Dusicka and Iwai, 2007; Dusicka and Lewis, 2010; Malakoutian et al., 2013). This structural system consists of a steel frame (LC) with replaceable link beams which acts as a fusion element to increase the seismic performance. Figure 1 shows a general view of the LCF system.

In the structural systems which are combined with these fuses, the damage in the main members is limited and the ability to

easily and quickly replace the damaged fuses will reduce the time and cost of repairing the building. Nowadays, the concept of fuse has changed. In the past, the main purpose of fuse members was to dissipate the seismic energy by the inelastic deformations, and they were not necessarily replaceable.

Since the LCF system has included two structural systems based on the interconnection between the two fusel structures and the main structure, the linked beams are responsible for fuses. Inelastic deflection and yielding are formed only in the linked beams, and the members of the main structure should remain elastic phase. Design and seismic performance of steel MRFs incorporating replaceable fuses was studied and evaluated by Shen et al. (2011). The results indicate that steel MRFs with replaceable links, possess a suitable ductility with the added coup that the link can be replaced with after an earthquake.

Shoeibi et al. (2017) introduced an iterative, simple and highly accurate procedure for designing these dual systems using the Performance-Based Plastic Design method (PBPD). This method was based on separating the two structural systems considering their interactions. In addition, they designed three structures with 3, 6 and 9 stories with this method. To evaluate the proposed method, nonlinear static and dynamic analysis was applied. The results showed that the designed structures achieved the performance objectives.

Lia et al. (2018) proposed a novel system of steel Energy-Dissipative Columns (EDCs) to mitigate seismic responses of reinforced concrete MRFs. The results showed that the lateral stiffness ratio of EDC to MRF, the story irregularity factor of MRFs, and the ratio of story shear capacity of EDC-MF systems to seismic base shear are the most important parameters.

The purpose of this study is to investigate the effect of link beam length in the LCF system for the seismic retrofit RC frame. For the first time, this system has been used to retrofit the RC frame. Therefore, determination of ratio of link beam length to the span length of the RC frame can increase the LCF system efficiency for retrofit of the RC frame. Therefore, the plastic hinges are first formed in the link beam of the LC frame and the main structure remains (RC frame) in the elastic phase to maintain the serviceability of the structure.

VERIFICATION OF FINITE ELEMENT MODEL

In this study, the experimental investigation of Choi and Park (2008, 2011) has been used for the verification of a nonlinear Finite Element (FE) model with ABAQUS 6.14-5.

Description of Tested Specimen by Choi and Park and FE Model for RC Frame

In this paper, the experimental specimen was one-third scale specimen of three-story RC frame which has been studied by Choi and Park (2011). The LCF system is used for retrofitting the RC frame. The dimensions and reinforcement details of the tested specimen by Choi and Park (2011) are shown in Figure 2.

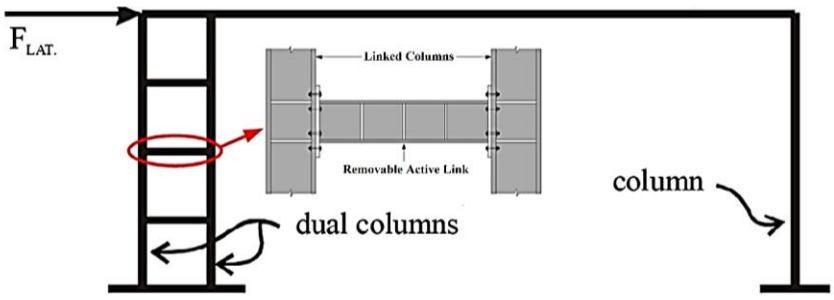

Fig. 1. Concrete or steel frame retrofitted with the LCF system (Lia et al., 2018)

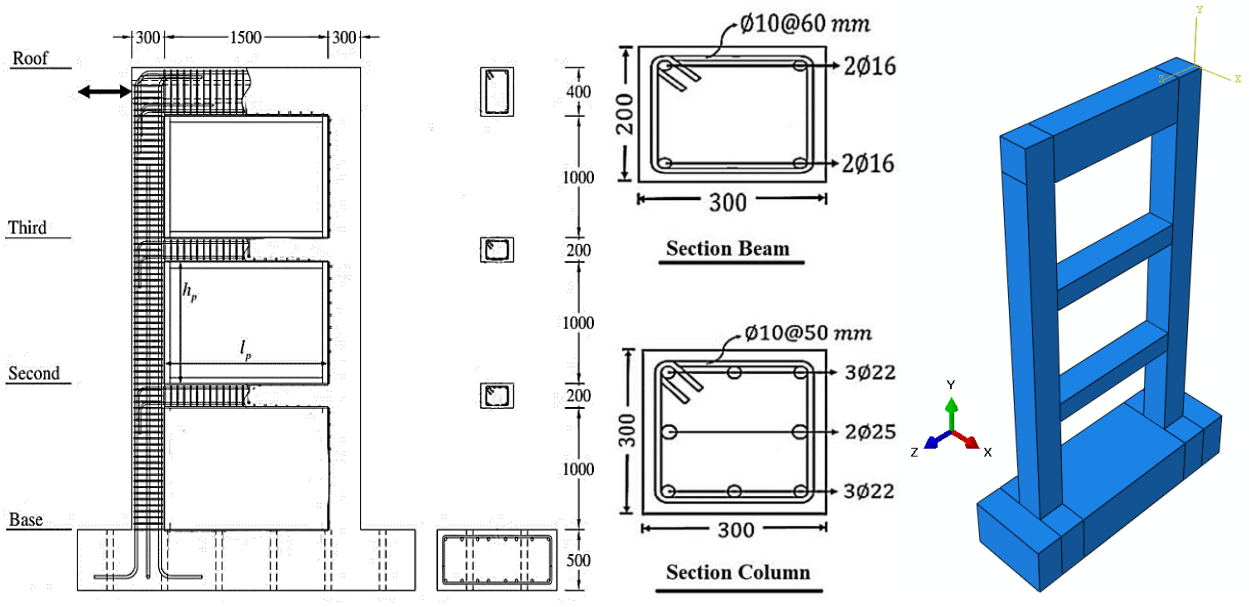

(a) (b)

Fig. 2. Dimensions and reinforcement details of the RC frame (Choi and Park, 2011): a) Tested specimen (Choi and Park, 2011); b) FE model

The properties of the tested specimen are listed in Tables 1 and 2. The RC frame was designed in accordance with building code requirements for structural concrete (ACI 318-14). The aspect ratio (l_p/h_p) was 1.5 (l_p = 1500 mm and h_p = 1000 mm, where l_p and h_p are the length and height of the RC frame, respectively).

The mechanical behavior of concrete has been used the concrete damaged plasticity model. The specifications of concrete damaged plasticity for the FE model are summarized in Table 3. The elements of the RC frame use a three-dimensional 8-node hexahedral elements with reduced integration (C3D8R) to prevent the shear locking effect. In order to model reinforcements, 2-node truss elements (T3D2) having 3 degrees of freedom at each node (translations in X, Y and Z directions of global coordinate system) are used. To define the interaction between concrete and reinforcements, embedded region interaction is used.

Table 1. Properties of material tested specimen for RC frame

Material	Poisson's ratio	Modulus of elasticity (MPa)	Compressive strength (MPa)	Tensile strength (MPa)
Concrete	0.15	25000	26.4	-
Steel	0.3	200000	-	400

Table 2. Properties of tested specimen for the RC frame

	Area (mm^2)	Yield strength (MPa)
Longitudinal reinforcement of column	506.7 (D25)	443
	387.1 (D22)	430
Longitudinal reinforcement of beam	198.1 (D16)	471
Transverse reinforcement	71.3 (D10)	486

Table 3. Specifications of concrete damaged plasticity for concrete

Dilation angle	Eccentricity	Fb0/Fc0	K	Viscosity parameter
31	0.1	1.16	0.667	0.002

It is important to choose the appropriate mesh size for accurate verification of the RC frame tested specimen with the FE model. To achieve accurate results at the optimum time, sensitivity analysis is performed for the mesh size. The steps of sensitivity analysis for the RC frame are listed in Table 4.

Figure 3 shows the deformations of the RC frame for the tested specimen and the FE model under a monotonic displacement controlled lateral load pattern which continuously increases.

Figure 4 shows the verification of the pushover curve of the tested specimen with the FE model, which selected mesh size of FE model for the RC frame. The mesh size of concrete and bar is equal 110 mm, 30 mm, respectively (FE model of RCF = BAR 30, RC110). This size of the meshes has good agreement with the experimental specimen results.

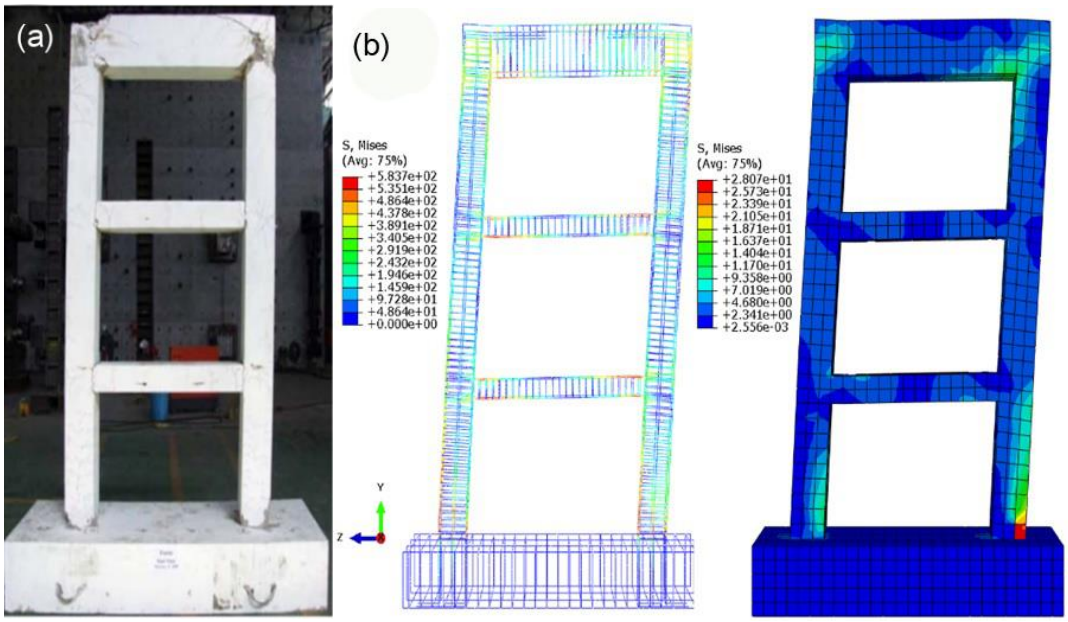

Fig. 3. The deformation of the RC frame in the ultimate displacement: a) The deformation of experimental specimen (Choi and Park, 2011); b) Von Mises stress of RC frame in the FE model

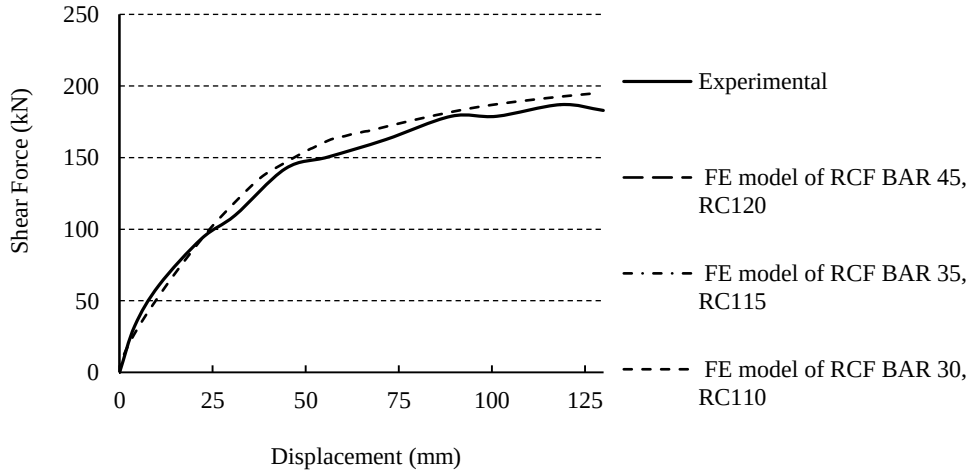

Fig. 4. Verification of the tested specimen with the FE model for the RC frame

Table 4. Size and type of mesh element in the FE model of RC frame

	Element type	Element size (mm)	
Concrete	C3D8R	Step 1	120
		Step 2	115
		Step 3	110
Longitudinal & Transverse reinforcement	T3D2	Step 1	45
		Step 2	35
		Step 3	30

Description of Tested Specimen by Choi and Park and the FE Model for Steel Frame

To verify the FE model for steel frame, a one-third model is used in an experimental study Choi and Park (2008). The configuration of the specimen tested by Choi and Park (2008) is presented in Figure 5. The frame members are built-up sections made of SM490 steel (F_y = 330 MPa). All columns were H-150×150×22×22 mm (built-up wide flange section, H-overall depth (dc) × flange width (bf) web thickness (t_w) × flange thickness (t_f)). The beams in the second and third stories are H-150×100×12×20. The top beam that connects to the actuator is H-250×150×12×20.

The FE model for the steel frame elements in ABAQUS software has been used the S4R element. The S4R element is a 4-node, quadrilateral, stress or displacement shell element with reduced integration and a large-strain formulation. To achieve accurate results at the optimum time, sensitivity analysis for mesh size is performed. Table 5 shows the steps of the sensitivity analysis for choosing the mesh size of the FE model for the steel frame.

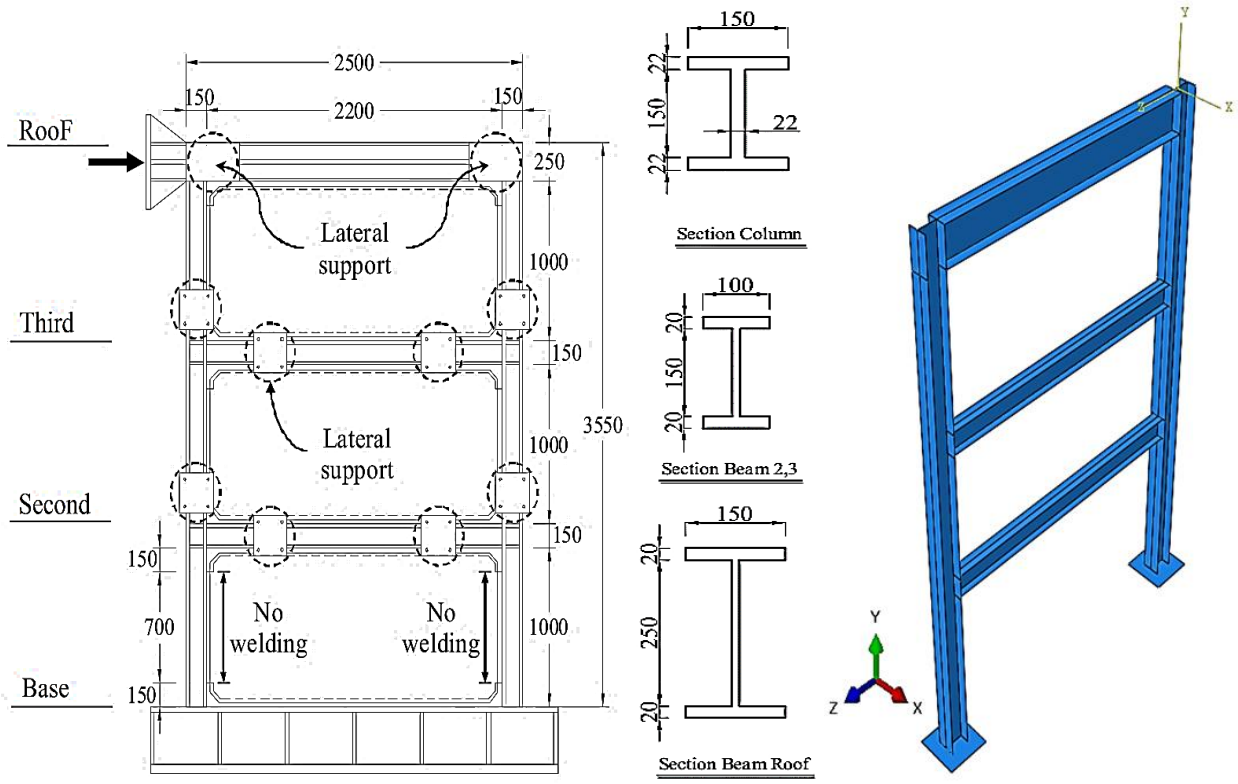

(a) (b)

Fig. 5. Dimensions of the steel frame (unit: mm): a) The tested specimen (Choi and Park; 2008); b) The FE model

Table 5. Size and type element of the FE model for the steel frame

Element type	Element size	
S4R	Step 1	60
	Step 2	50
	Step 3	40

Figure 6 shows the verification of the pushover curve for the experimental specimen and the FE model. A uniform mesh size of 40 mm is chosen for the steel frame elements as shown in Figure 7.

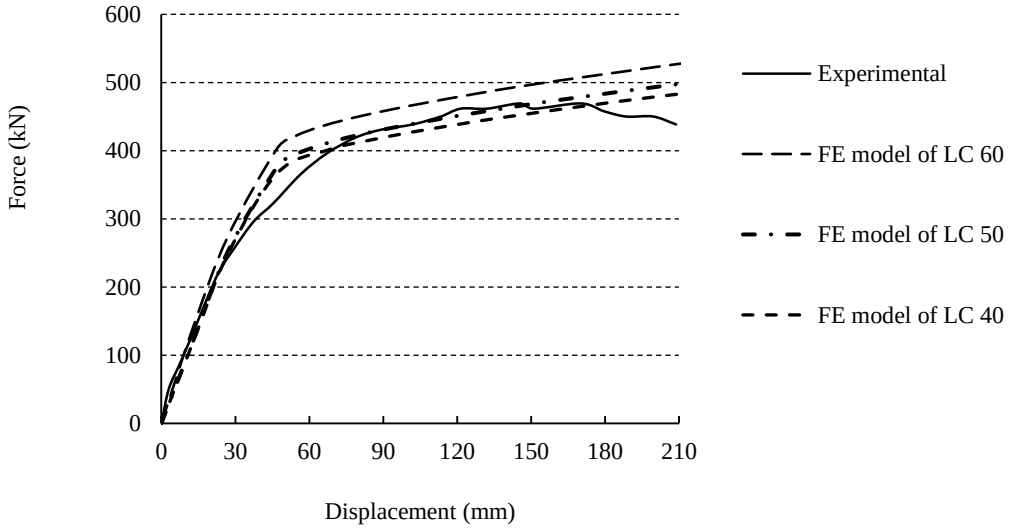

Fig. 6. Verification of the experimental specimen and the FE model for the steel frame

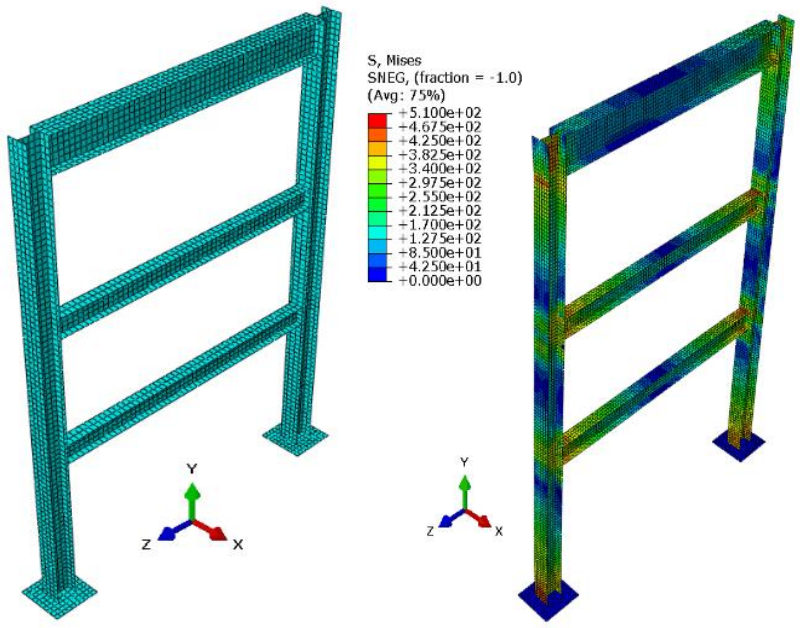

(a) (b)

Fig. 7. The deformation of the steel frame in the ultimate displacement: a) The element mesh; b) Von Mises stress

Description of the FE Model

The design of the columns of the LC frame is calculated using the virtual work method for the maximum shear force corresponding to the first plastic hinge in the members of the RC frame obtained from the nonlinear static analysis. The lateral displacement considering flexure is only obtained using the equation of virtual work as follows.

$$\Delta = \int_0^L \frac{Mm}{EI} \qquad (1)$$

where *M*: is the internal moment caused by the real load, *m*: is the internal moment caused by the external virtual unit load, *E*: is the modulus of elasticity and *I*: is the moment of inertia.

The design of the link beams of the LC frame is calculated using the slope-deflection method. The beam links are designed in accordance with seismic provisions for structural steel buildings (ANSI/AISC 341-10). In this paper, retrofitting of the RC frame is investigated using the LCF system for nine different lengths of link beams. All columns and link beams section of the steel frame (LC frame) are designed IPB 280 and IPE 160, respectively. Figure 8 shows the dimensions of the RC frame is retrofitted using the LCF system and how to connect the LC frame to the RC frame. The naming of the models follows the concept of LCF which represents the LCF system in which the first number after the LCF is the length of the link beam (unit: meters) and the second number is the ratio of the link beam length to the span length of the RC frame. The span length of the RC frame for all models is 1.8 m. Naming and the link beam length for different models are summarized in Table 6. For comparability of the results, material properties, meshing, boundary conditions and the diameter of the bars of all models are considered the same as those of the experimental specimen tested by Choi and Park (2011).

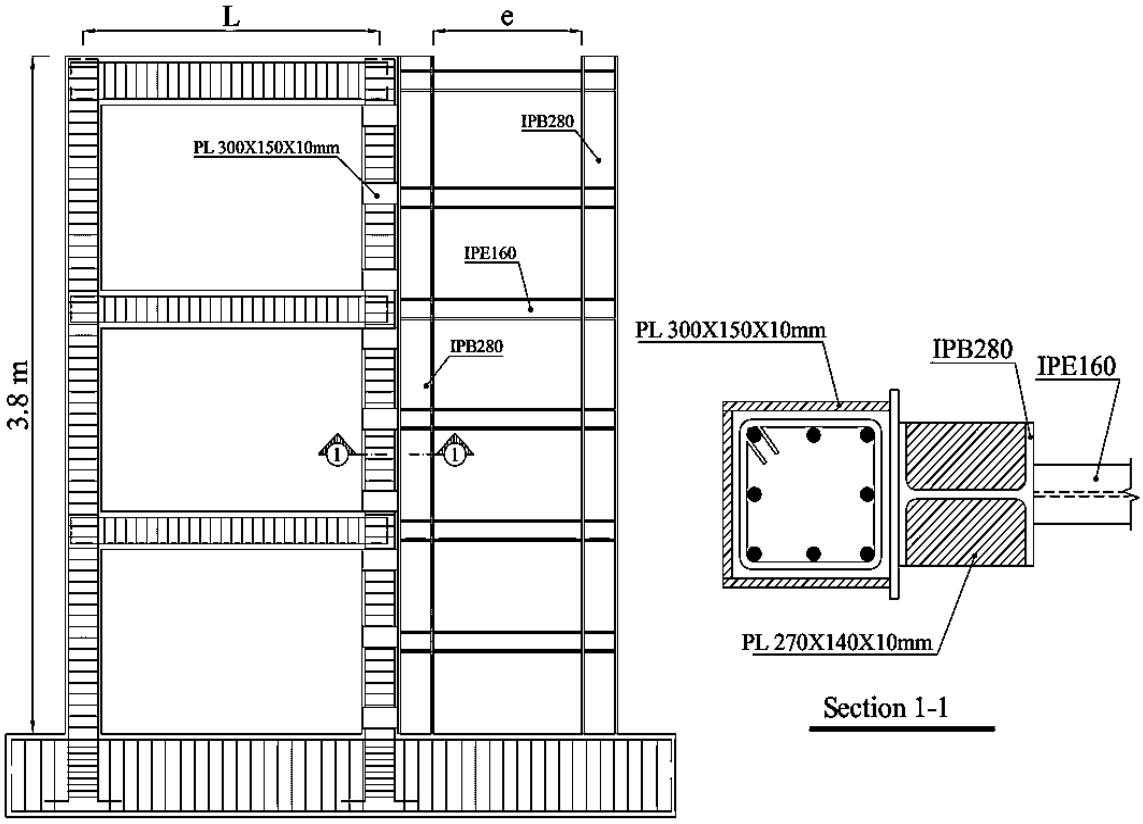

Fig. 8. The RC frame retrofitting with LCF system

Table 6. Naming and link beam length for different models

Model	e (m)	e/L
LCF-0-0	0	0
LCF-0.3-0.15	0.3	0.15
LCF-0.55-0.3	0.55	0.3
LCF-0.8-0.45	0.8	0.45
LCF-1.1-0.6	1.1	0.6
LCF-1.35-0.75	1.35	0.75
LCF-1.8-1	1.8	1
LCF-2.25-1.25	2.25	1.25
LCF-2.7-1.5	2.7	1.5

The Interaction between the RC and the LC Frame

To define the interaction between concrete and reinforcements in the RC frame is used embedded region interaction in the finite element software ABAQUS. For connecting the steel plate of the LC frame to the foundation, a tie constraint is used. This constraint ties two separate surfaces together so that there is no relative motion between them. This type of constraint allows to fuse two regions together, even though the meshes created on the surfaces of the regions may be dissimilar. U-shaped constraints are used to define interactions between the LC frame and the RC frame is used (Bypour et al., 2019), as shown in Figure 9.

The surface-to-surface contact interaction is used in the finite element software Abaqus to define interactions between the RC frame and LC frame. A contact interaction property can be referred to as the general contact, surface-to-surface contact, or self-contact interaction. Normal and tangential behavior is considered in the interaction element. The friction coefficient defined is equal to 0.18.

Loading

The loading process for studying the LCF system was controlled by displacement at the top beam. The displacement which was equal to the maximum target displacement of experimental test was applied in non-linear Finite Element Analysis (FEA). For this purpose, the FEA of the LCF system has been performed in a nonlinear static analysis format and the analysis procedure has been considered both material and geometric nonlinearities. The boundary conditions of the LCF model are shown in Figure 10a.

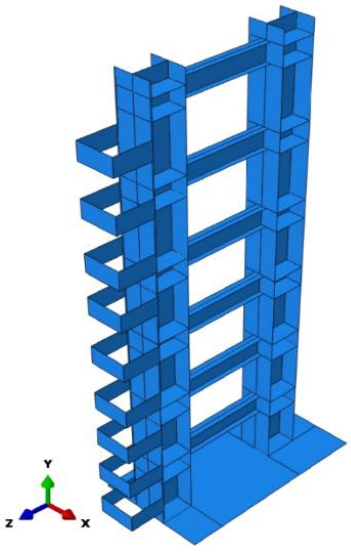

Fig. 9. Connecting the LC frame to the RC frame using U-shaped constraints

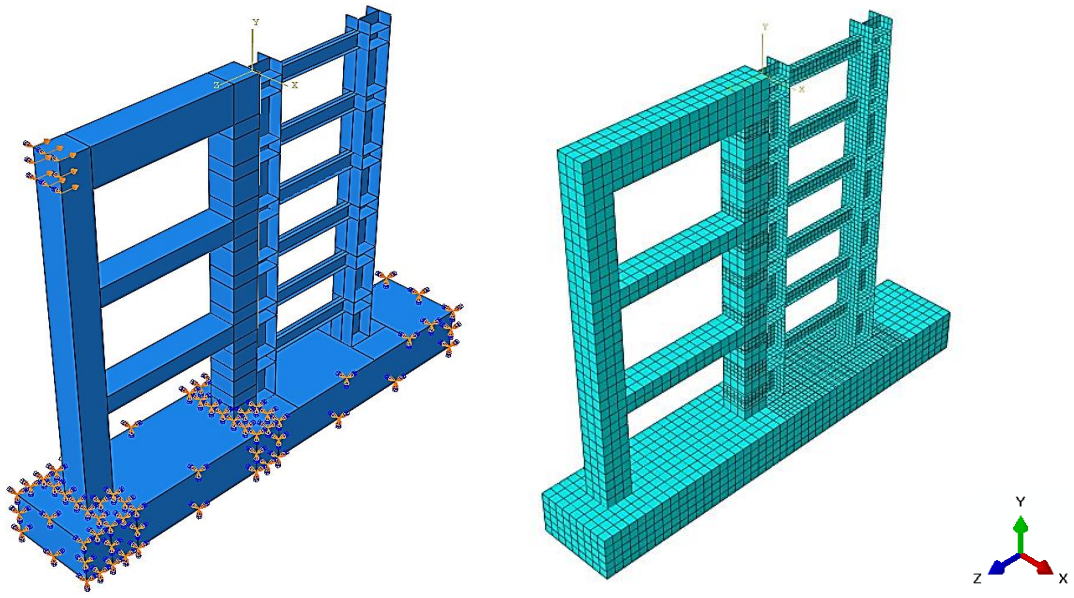

(a) (b)

Fig. 10. FE model of the LCF system: a) The boundary conditions; b) meshing

RESULTS AND DISCUSSION

Investigation of Pushover Analysis Procedure for Models

The capacity curve represents the shear tolerability by the structure since the area under the curve of force-displacement (pushover) shows the dissipated energy by the structure. Whatever the surface below this curve is larger, the structure has more ability for energy absorption and force redistribution. When the structure is under the influence of large forces caused by an earthquake, if it has an elastic behavior, it is able to dissipate the input energy from the earthquake. Figure 11 shows the comparison of the results of the force-displacement curve of all models for retrofitting of the RC frame.

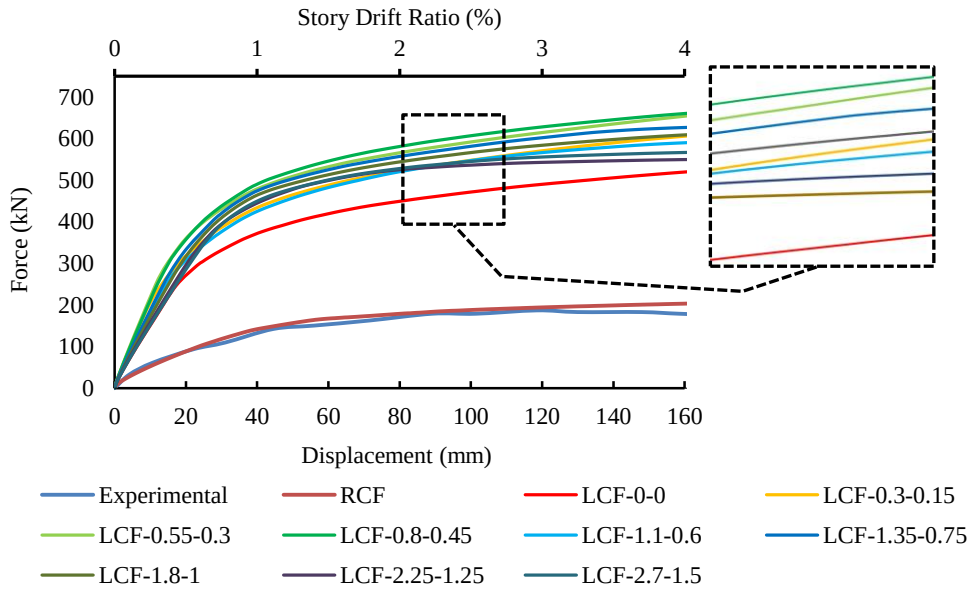

Fig. 11. The comparison results of the force-displacement curve on all models

The link beams in the LC frame are designed to yielding dissipate the energy absorbed by the structure and the members of the RC frame remain in the elastic phase. The maximum ultimate load is created in the model of LCF-0.55-0.3 and LCF-0.8-0.45. Consequently, the capacity of the LCF system compared to the primary frame (without retrofitting) is increased about 3.2 as shown in Figure 11. To avoid density of the curves and provide more precise interpretation of each model, the pushover curve for each model is examined separately in order to study the formation of plastic hinges progress in the LCF system with different lengths of the link beam.

The Formation of Plastic Hinge Progress in the LCf System

The formation of plastic hinges in the RC and the LC frame under increasing lateral load is shown in Figure 12. The plastic hinges formation in the LCF system are first formed in the link beam and the columns of the LC frame and then in the beams and columns of the RC frame. This causes the RC frame remains in the elastic phase and does not damage the main moment frame (the RC frame) in severe earthquakes. For naming, the plastic hinge of the beam is introduced by the letter B and the plastic hinge of the column by the letter C, as shown in Figure 12. For example, B-LC represents a plastic hinge formation in the link beam of the LC frame and B-RCF represents the plastic hinge in the beam of the RC frame (without retrofitting). The naming formation of plastic hinges is summarized in Table 7.

Table 7. Naming of plastic hinges in the LC and the RC frame

Naming of plastic hinges	Place of plastic hinge formation
B-LC	The link beam of LC frame
C-LC	The column of LC frame
B-RC	The beam of RC frame
C-RC	The column of RC frame
B-RCF	The beam of RC frame (without LCF system)
C-RCF	The column of RC frame (without LCF system)

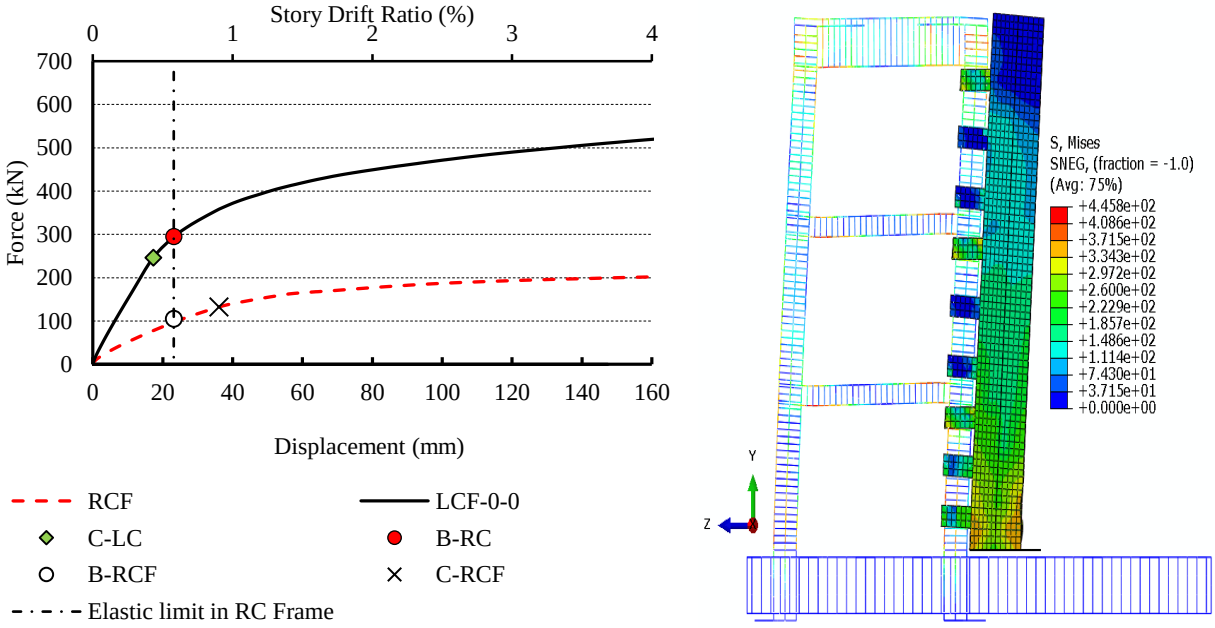

(a) Model: LCF-0-0

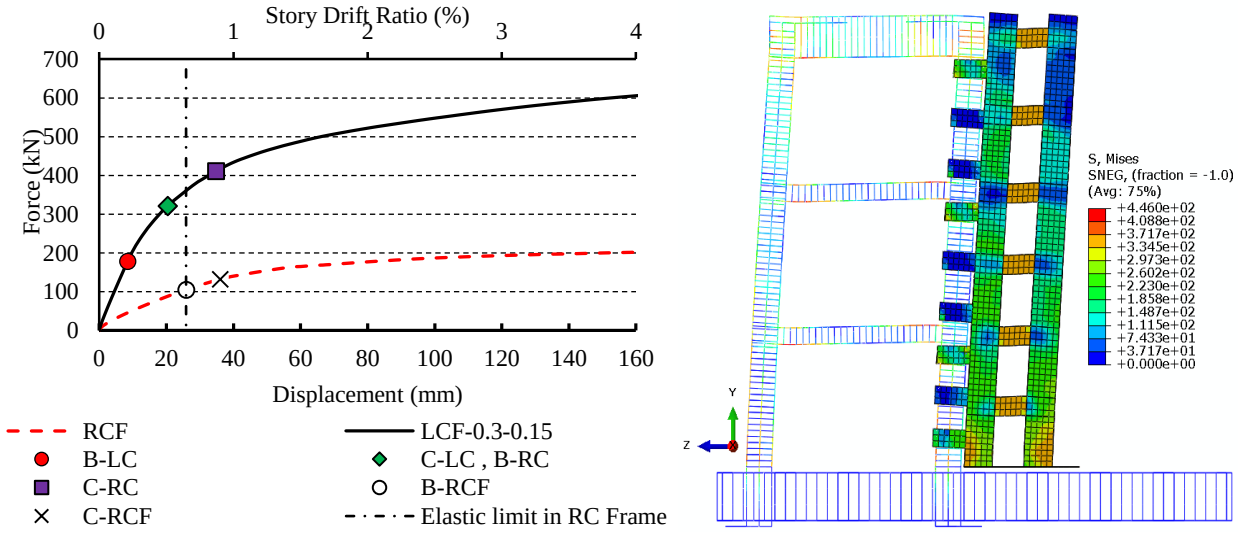

(b) Model: LCF-0.3-0.15

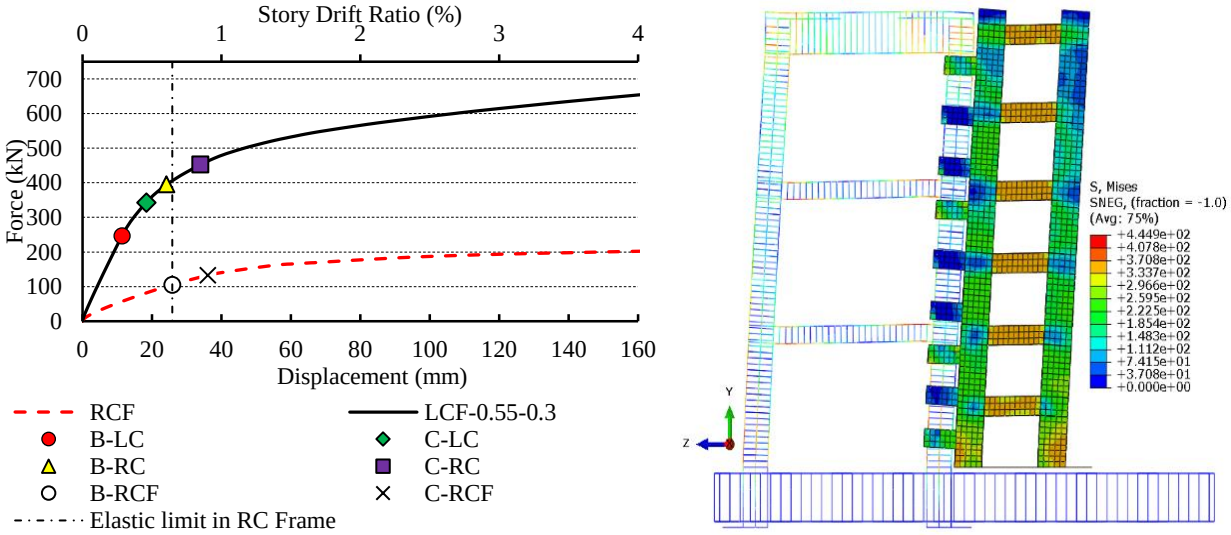

(c) Model: LCF-0.55-0.3

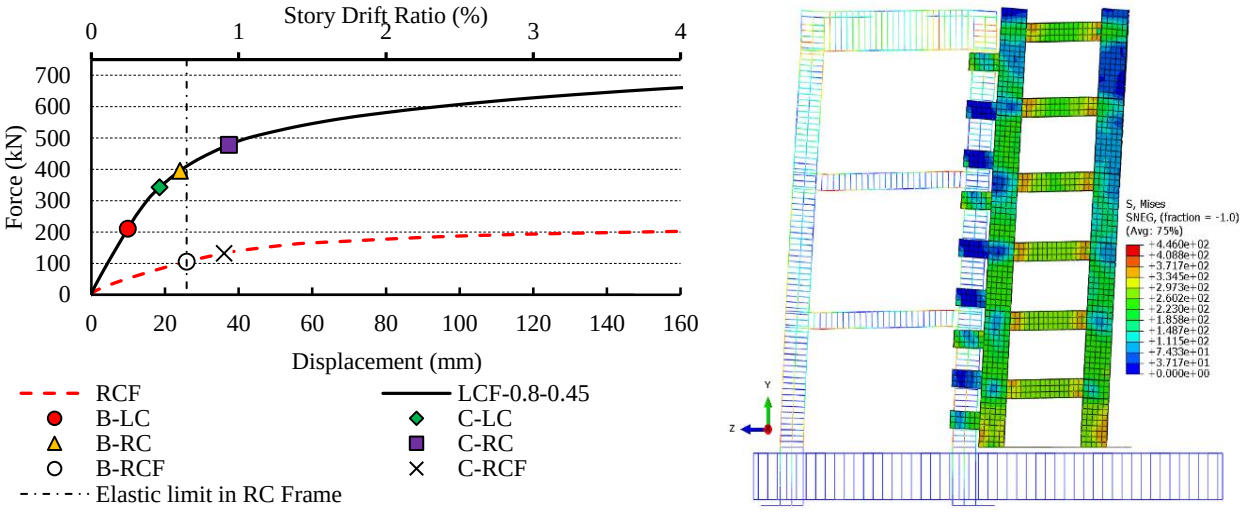

(d) Model: LCF-0.8-0.45

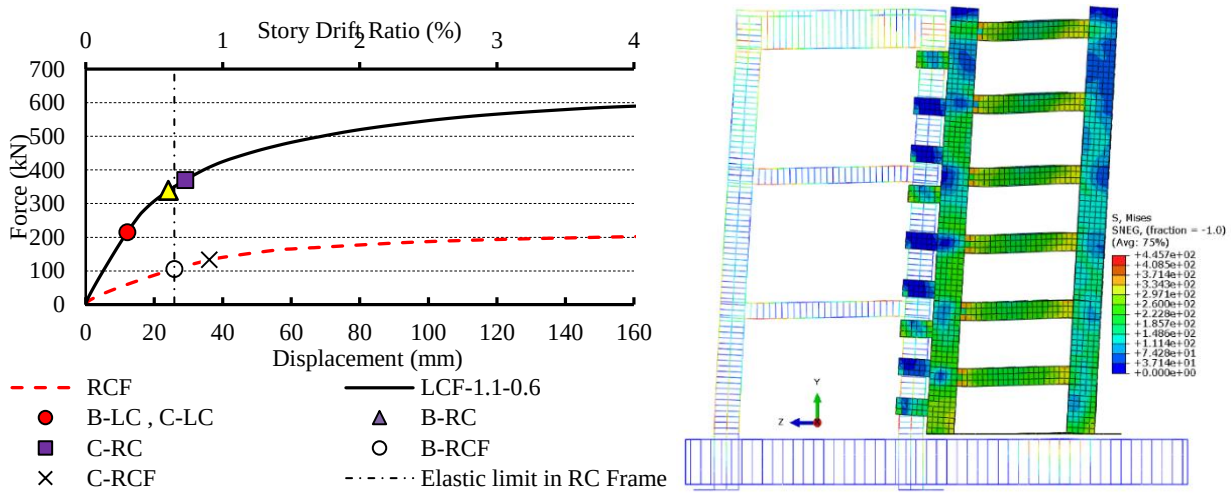

(e) Model: LCF-1.1-0.6

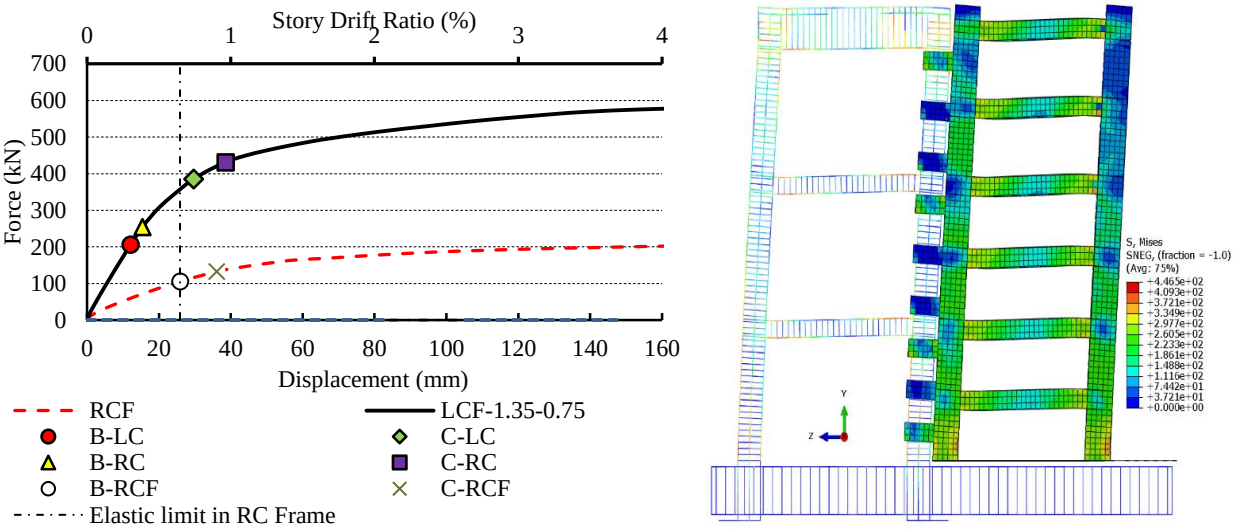

(f) Model: LCF-1.35-0.75

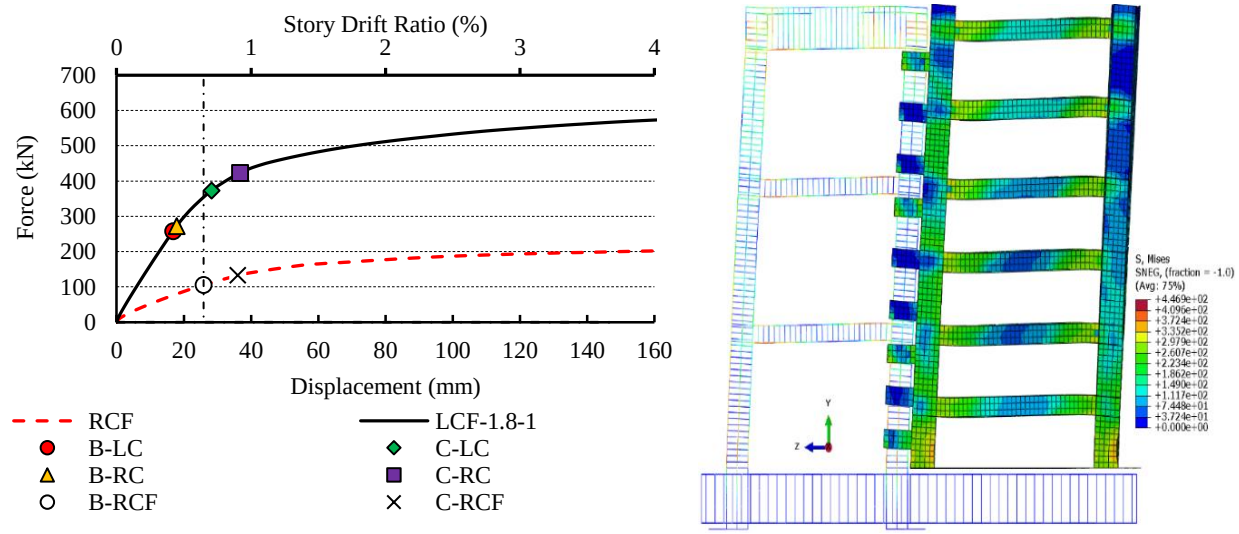

(g) Model: LCF-1.8-1

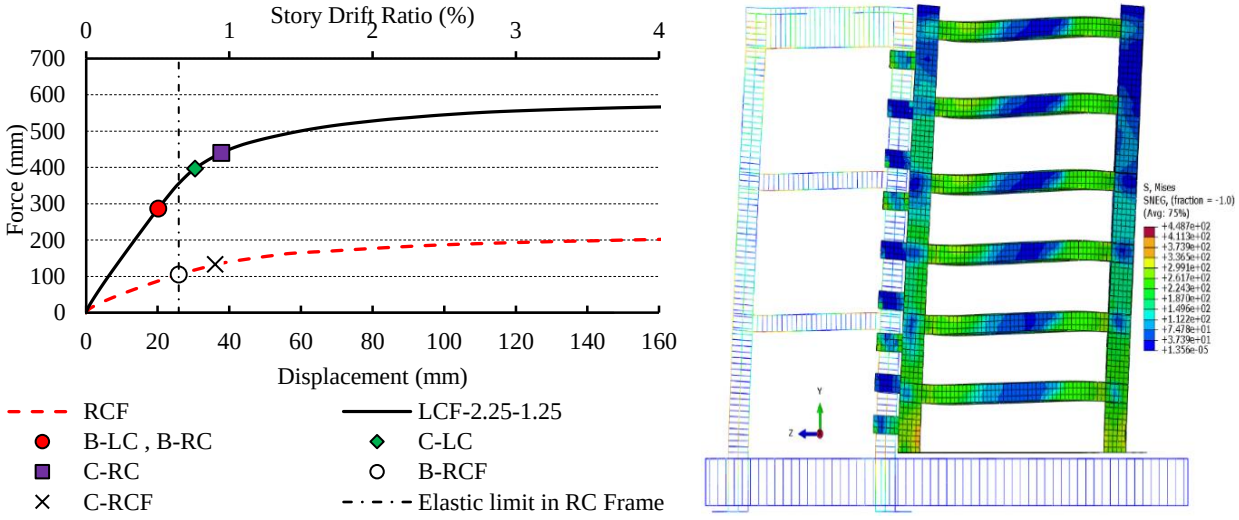

(h) Model: LCF-2.25-1.25

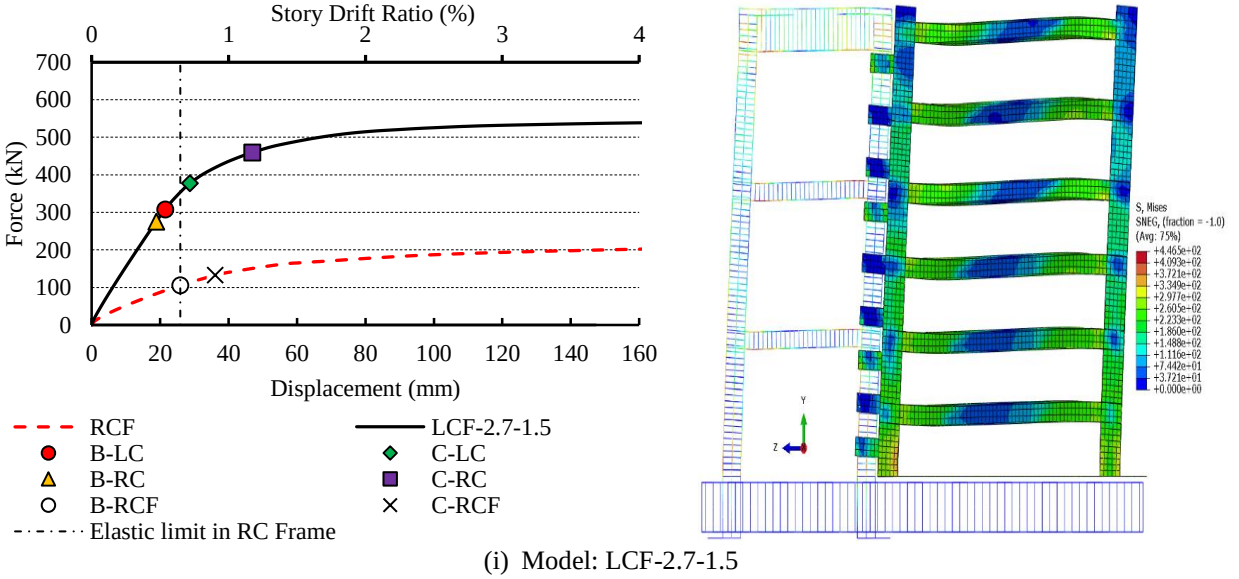

(i) Model: LCF-2.7-1.5

Fig. 12. The process of the plastic hinge formation in models with different lengths of link beam in the LCF system

As illustrated in Figure 12, the LCF-0-0 model, the ratio length of the link beam to the span length of the RC frame is equal to zero (e/L = 0). It means that, in this model only two columns of the LC frame are connected and there is no link beam. In the model of LCF-0-0, the plastic hinge is first formed in the frame of the LC frame and then the plastic hinges are formed in the beam and column of the RC frame. In the LCF-0.3-0.15 model, at first the plastic hinges are formed in the RC frame, then they are formed in the LC frame. It means that, the RC frame does not remain in the elastic phase. In the models of LCF-0.55-0.3 and LCF-0.8-0.45 the plastic hinges are initially formed in the LC frame and then in the RC frame.

In these two models, before that the members of the RC frame (beam and column) reach the yielding stress, the plastic hinges are initially formed in the link beams and then in the columns of the LC frame. The first plastic hinge in the LCF-0.55-0.3 model is the displacement of 11.40 mm (0.3% drift ratio) and the displacement of the LCF-0.8-0.45 model occurred at 9.93 mm (0.26% drift

ratio). The farther the distance between the formation of the first plastic hinge in the link beam of the LC frame and the formation of the first plastic hinge in the beams of the RC frame, the more potential the LCF system has to withstand the earthquake without damaging the member of moment frame (RC frame).

The model of LCF-1.1-0.6 first formed the plastic hinge in the LC frame and then formed the plastic hinge in the RC frame. The first plastic hinge is formed simultaneously in the link beams and columns of the LC frame at the displacement of 12.14 mm (0.34% drift ratio) and then the plastic hinges are formed in the RC frame at the displacement of 29.05 mm. The formation of plastic hinges in the models of LCF-1.35-0.75, LCF-1.8-1, LCF-2.25-1.25 and LCF-2.7-1.5 has not been properly appeared. The plastic hinges are first formed in the RC frame and then in the LC frame while the plastic hinges must be first formed in the LC frame and remains the RC frame in the elastic phase. Therefore, the formation of plastic hinges in the models of LCF-0.55-0.3, LCF-0.8-0.45 and LCF-1.1-0.6 is correctly observed.

The Link Beam Behavior in the LCF System

The link beams behavior of the LCF system is similar to the behavior of the EBF and the type of link beam yielding depends on its length and cross section. In the LCF system, selecting the type of the link beam depends on the structure height and the ratio of strength between the RC and LC frame. Kasai and Popov (1984) proposed ratio $\frac{Pu}{2Mp/h}$ versus e/L for a beam of the EBF. In this relation, h: is the height of the floor and P_u and M_p: are the ultimate load and the plastic moment of link beam, respectively. The ratio $\frac{Pu}{2Mp/h}$ versus e/L for the LCF system are shown in Figure 13.

As shown in Figure 13, by increasing the length of the link beam, the ultimate strength of the LCF system is reduced. Therefore, the ultimate strength of the LCF-0.8-0.45 model than the LCF-1.8-1 model has decreased about 60%. Also, the deformation of the link beam is effective on the behavior of the frame in inelastic phase. Figure 14 shows the ideal displacement of the link beam in the LCF system. When the link beam due to shear force reaches the limit of its yielding then the plastic mechanism is in accordance with Figure 14. Using this figure and the simplified plastic theory, the relationship between the rotational angle of the link beam (γ_p) and the plastic relative deformation angle of the floor (θ_p) is calculated as follows:

$$\gamma_p = \frac{L}{e}\theta_p \qquad (2)$$

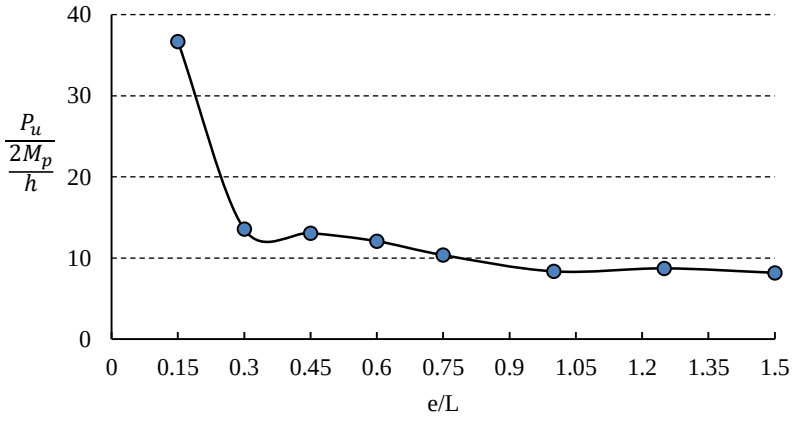

Fig. 13. The variation curve $\frac{Pu}{2Mp/h}$ vs *e/L* for the LCF system

Since the elastic deformation component is very small in comparison with the total displacement, therefore, the plastic relative deformation angle of the floor (θ_p) is calculated as follows:

$$\theta_p = \frac{\Delta_s}{h} \quad (3)$$

where Δ_s: is the maximum story displacement and h is the height of the floor. According to Eqs. (2) and (3), the amount of variation $\frac{\gamma_p}{\theta_p}$ in terms of *e/L* is shown in Figure 15.

As shown in Figure 15, the rotation angle value of the link beam for a short length (e/L = 0.15) is about 7 times higher than long length (e/L = 1.5). It causes the rotation at the end of the link beam to occur due to plastic deformation and create the plastic hinges in the LC frame. The amount of the link beam rotation in LCF-1.35-0.75, LCF-1.8-1, LCF-2.25-1.25 and LCF-2.7-1.5 models is very small. It means that, because of the plastic deformation, the first plastic hinges occurred in the moment frame (RC frame) and then the plastic hinges are formed in the LC frame.

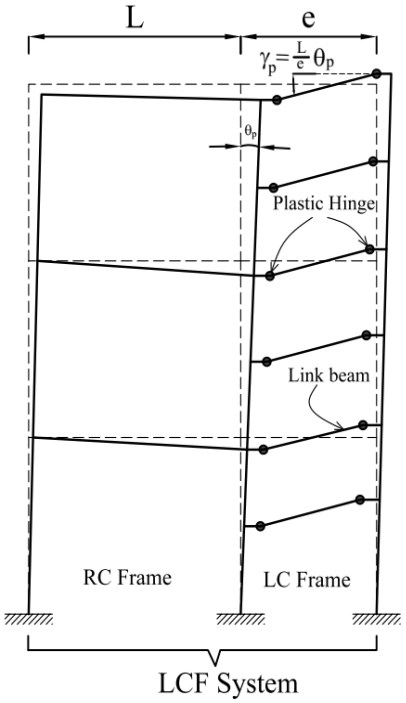

Fig. 14. The ideal displacement of the link beam in the LCF system

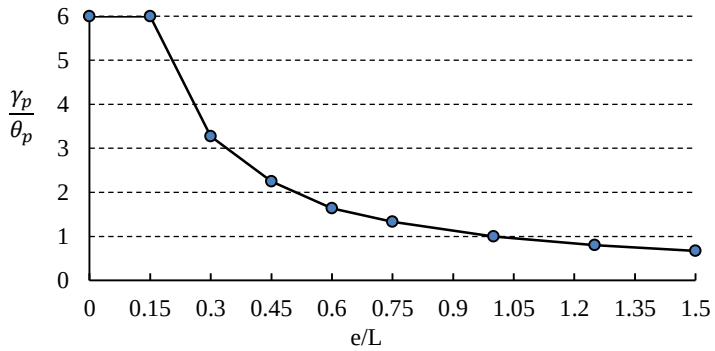

Fig. 15. The amount of rotation angle of the link beam for different lengths

Determining the Elastic Stiffness for the LC, RC, and LCF Systems

The elastic stiffness is calculated from the ratio of the base shear to the roof displacement in the elastic analysis. The elastic stiffness values in the LCF system made up of structures with LC and RC frames are calculated by Eq. (4).

$$K_{LCF}=\frac{V_{yLCF}}{\Delta_{yLCF}}, K_{LC}=\frac{V_{yLC}}{\Delta_{yLC}}, \quad K_{RC}=\frac{V_{yRC}}{\Delta_{yRC}} \Rightarrow K_{LCF}=K_{LC}+K_{RC} \tag{4}$$

where $V_{y\,RC}$, $V_{y\,LC}$ and $V_{y\,LCF}$: are the lateral elastic force of RC, LC and LCF systems, respectively, K_{LCF}, K_{LC} and K_{RC}: are the elastic stiffness of the systems LCF, LC, RC, respectively and $\Delta_{y\,LCF}, \Delta_{y\,LC}$ and $\Delta_{y\,RC}$: are the roof lateral displacement of the systems LCF, LC and RC, respectively.

The elastic stiffness for nine models is calculated in accordance with Eq. (4). The story shear force in proportion to elastic stiffness for RC and LC frame is distributed. The elastic stiffness for nine models versus the ratio of link beam length to the span length of the RC frame (e/L) are shown in Figure 17. The results of this curve are related to shear force and the corresponding displacement for the first plastic hinge is formed in the LCF system. For example, Figure 17 refers to LCF-0.8-0.45 model, which shows the amount of shear force in proportion to their relative stiffness is distributed between the RC and LC frame.

The more the elastic stiffness of the LC frame is, the more the ability of the structure will be to dissipate the lateral forces by the LC frame. The results of Figure 16 show, the highest elastic stiffness of the LC system is relevant to models of LCF-0.55-0.3 and LCF-0.8-0.45. The elastic stiffness ratio of the LC frame to the whole system stiffness (LCF system) for models LCF-0.55-0.3 and LCF-0.8-0.45 is about 90%. This will cause be the RC frame remains in an elastic phase and plastic hinges are first formed in the LC frame and then in the RC frame. By increasing the length of the link beam for the models, the elastic stiffness decreased about 75% in models of LCF-1.35-0.75, LCF-1.8-1, LCF-2.25-1.25 and LCF-2.7-1.5 compared with the models of LCF-0.55-0.3 and LCF-0.8-0.45. It means that, more shear force entered the RC frame as a result the first plastic hinges are formed in the RC frame and from the capacity of the RC frame is used to absorb and dissipate the energy.

Levels of Performance and Behavior of the LCF System

For seismic design based on the performance of structures with the structural fuse system is the performance-based plastic design, whose main key is the separation of the two systems based on the interaction between the structural fuse system and the main structure. The structural fuse system design is combined with the original structure, which includes three levels of performance. First performance objective: Immediate Occupancy, where all the fuse and structure members remain elastic in earthquakes with 50% probability of exceedance in 50 years. Second performance objective: Rapid Repair, where the fuse members enter inelastic phase and yield in earthquakes with 10% probability of exceedance in 50 years, while the main structure members remain elastic. In this performance objective, the fuse system must perform its primary function and protect the main structure members from yielding, and after replacement of the fuse members, the building should immediately return to occupancy. Third performance objective: Collapse Prevention, where all the fuse and ductile structure members are allowed to enter an inelastic phase in earthquakes with 2% probability of exceedance in 50 years.

The capacity curve of the dual structure system under the lateral load versus roof displacement is obtained by the addition of the capacities of the structural fuse system (LC) and the main structural system (RC) as shown in Figure 18.

According to Figure 18, in the LCF systems, $V_{y\,LCF}$ and $\Delta_{y\,LCF}$: are base shear force and the corresponding displacement for the first plastic hinge formed in the link beams of LC frame, respectively. $V_{p\,LCF}$ and $\Delta_{p\,LCF}$: are base shear force and the corresponding displacement for the first plastic hinge formed in the beams of RC frame, respectively. In the LCF structural system, the link beams should be designed due to seismic loads with yielding has the capability of absorption and dissipation energy and all members of the main structure (RC) remained in an elastic state.

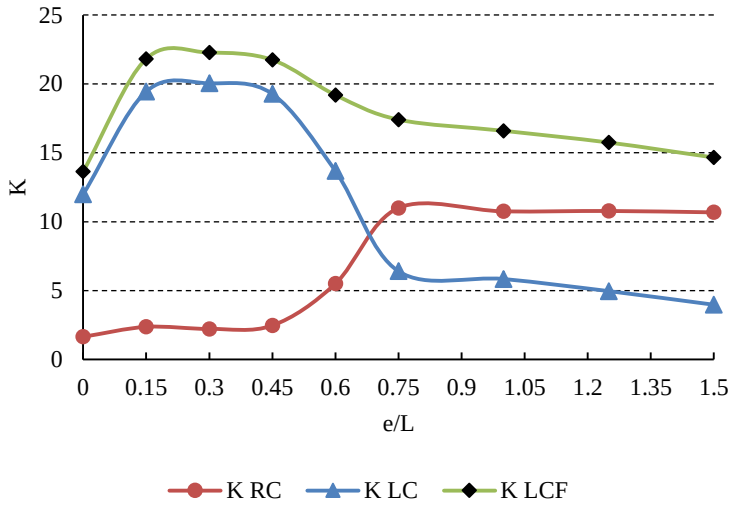

Fig. 16. The elastic stiffness value for nine models vs the ratio of e/L

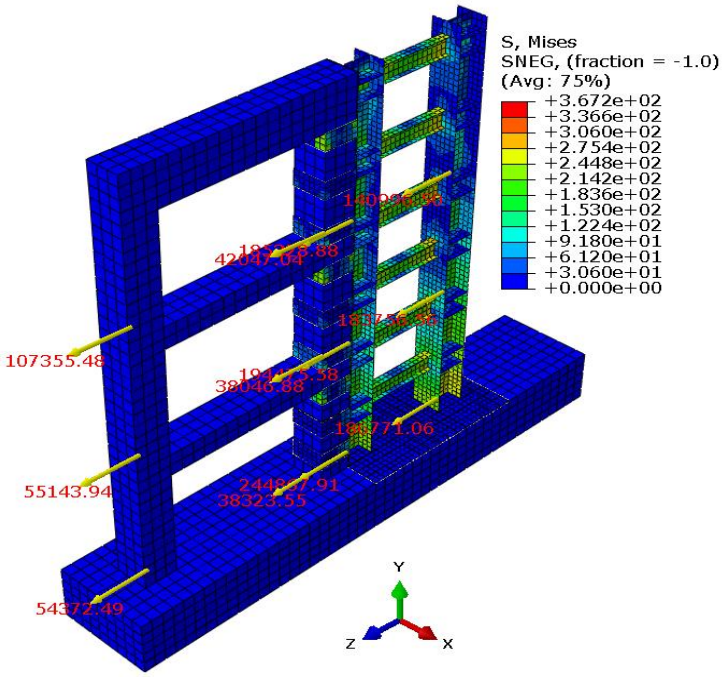

Fig. 17. The shear force in the RC and LC frames for LCF-0.8-0.45 model

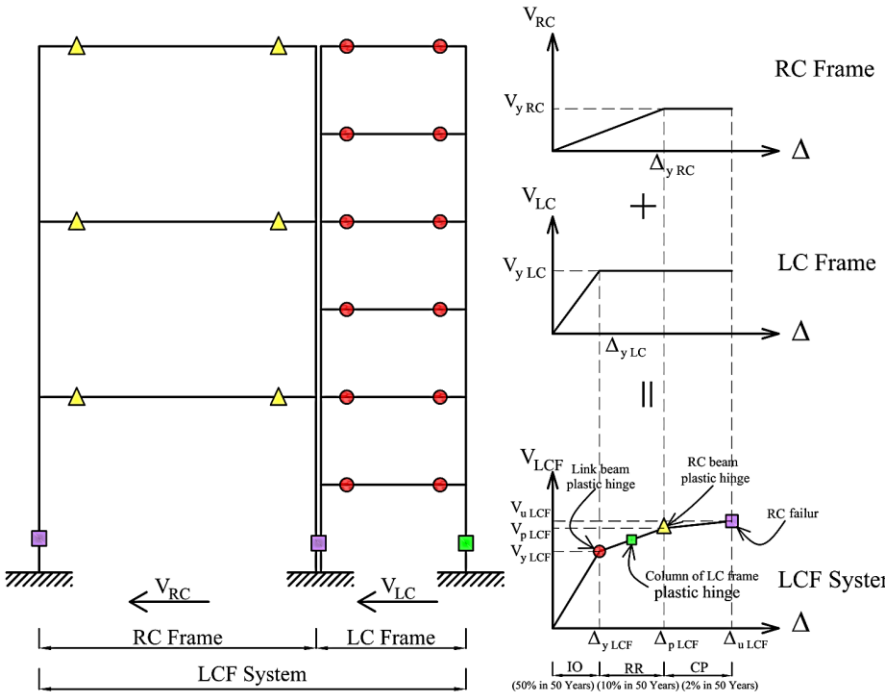

Fig. 18. The performance levels and the hazard levels of the LCF system on the component pushover curves

As shown in Figure 18, only the members of the link beam at the distance between $\Delta_{y\,LCF}$ and $\Delta_{p\,LCF}$ reaches the yield mechanism. Therefore, if the distance between $\Delta_{y\,LCF}$ and $\Delta_{p\,LCF}$ is more than each other, the LCF system has the potential to withstand earthquake without damaging the flexural members (RC frame). In this case, all damages will be limited to link beams that are replaceable and as a result the system will reach the performance level of RR to occupancy. The efficiency of the LCF system is a function of the ratio of $\Delta_{p\ LCF}$ to $\Delta_{y\ LCF}$. This ratio proposed by Malakutian et al. (2016) as the primary condition for design of LCF system and performance-based assessment as shown in Eq. (5).

$$1.2 < \frac{\Delta_{pLCF}}{\Delta_{yLCF}} < 3 \qquad (5)$$

If this ratio is less than 1, as a result the system lacks potential to access to the Rapid Repair (RR) performance level and the concept of the fuse in this system is lost. If this ratio is close to three, it means that, this system will have the potential to reach the rapid return to occupancy performance level. For this purpose, models of LCF-0.55-0.3, LCF-0.8-0.45 and LCF-1.1-0.6 first form the plastic hinges in the LC frame and then RC frame and the members of RC frame remain in the elastic phase. The curve of force-displacement (pushover) for three models as shown in Figure 19.

In order to evaluate the efficiency of the LCF system for these three models, it is important to calculate the ratio Δ_{PLCF} to Δ_{yLCF} which is proposed by Malakoutian et al. (2016). According to the obtained results of Figure 18, the ratio of Δ_{PLCF} to Δ_{yLCF}, is presented in Table 8.

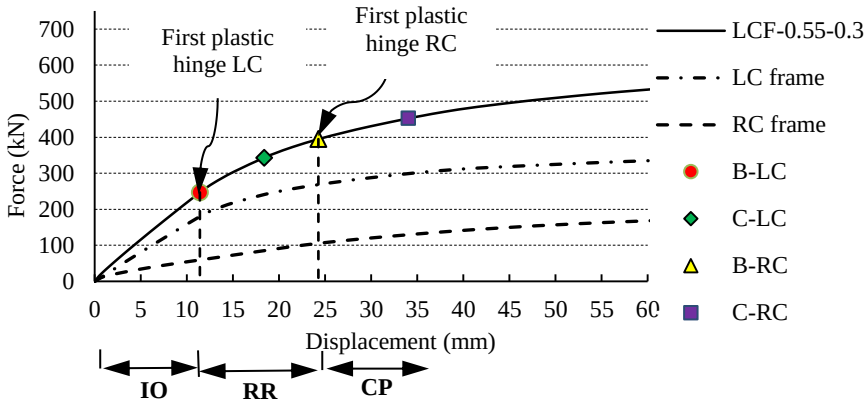

(a) LCF-0.55-0.3

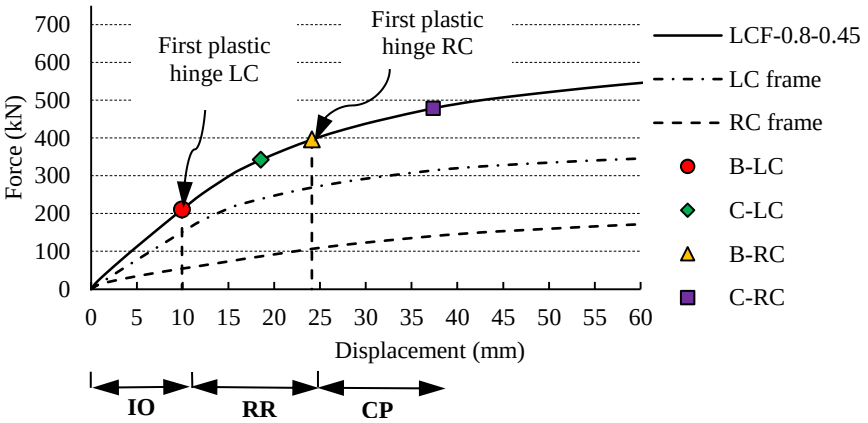

(b) LCF-0.8-0.45

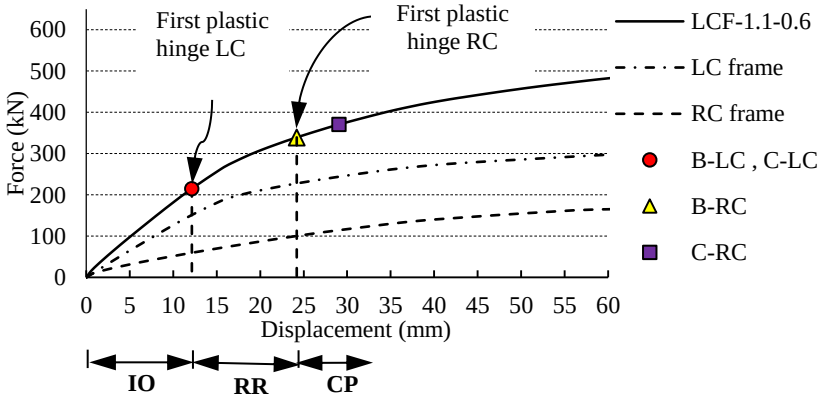

(c) LCF-1.1-0.6

Fig. 19. The curve of force-displacement of the LCF system

Table 8. The ratio of $\Delta_{p\ LCF}$ to $\Delta_{y\ LCF}$ and the ratio of $V_{p\ LCF}$ to $V_{y\ LCF}$

Model	$\Delta_{p\ LCF}$ (mm)	$Drift_{p\ LCF}$ (%)	$\Delta_{y\ LCF}$ (mm)	$Drift_{y\ LCF}$ (%)	$\Delta_{p\ LCF}/\Delta_{y\ LCF}$	$V_{y\ LCF}$ (kN)	$V_{p\ LCF}$ (kN)	$V_{p\ LCF}/V_{y\ LCF}$
LCF-0.3-0.15	24.26	0.674	11.4	0.32	2.13	246.802	394.671	1.49
LCF-0.8-0.45	24.11	0.67	9.93	0.28	2.43	210.484	395.642	1.88
LCF-1.1-0.6	24.23	0.673	12.14	0.34	2	215.179	339.232	1.57

As shown in Table 8, the ratio of Δ_{PLCF} to Δ_{yLCF} is increased in the model of LCF-0.8-0.45 than models of LCF-0.55-0.3 and LCF-1.1-0.6 about 14% and 22%, respectively. It means that, the LCF-0.8-0.45 model has more potential to reach the RR to occupancy performance level and preserve serviceability after an earthquake. Therefore, the model of LCF-0.8-0.45 is more in performance and efficiency than other models.

CONCLUSIONS

In this paper, nine models of LCF with different lengths of the link beam are investigated in order to retrofit the RC frame based on nonlinear static analysis procedure. The main findings obtained from this research are summarized as follows:

- In the models studied, models of LCF-0.55-0.3 and LCF-0.8-0.45 have the best performance and efficiency compared to other models. Because the formation of the plastic hinges in the LCF system is that the plastic hinges must be first formed in the link beams and columns of the LC frame and then it is formed in the beam and column of the RC frame. The formation of the plastic hinges, in these three models, is correctly observed.
- The degree of rotation of the link beam has an effect on the behavior of the LCF system in the inelastic range. The ratio of the plastic angle of the link beam (γ_p) to the relative plastic deformation angle of the floor (θ_p) is 2.25 for LCF-0.8-0.45 model. This ratio for the models of LCF-1.35-0.75, LCF-1.8-1, LCF-2.25-1.25 and LCF-2.7-1.5 is less than 1 which results in the plastic hinges to be first formed in the main frame (RC frame).As a result, it is best that the ratio of the plastic angle of the link beam (γ_p) to the relative plastic deformation angle of the floor (θ_p) to be limited between 2 to 3.5. Because the plastic hinges are first formed in the link beam and then in the column of LC frame, the RC frame remains in an elastic state and the link beams of the LCF act as a shear fuse and dissipate the earthquake energy.
- For the models of LCF-0.55-0.3 and LCF-0.8-0.45, the elastic stiffness ratio of the LC frame to the whole system stiffness (LCF system) is about 90%. The stiffness of the LC frame for models of LCF-1.35-0.75, LCF-1.8-1, LCF-2.25-1.25 and LCF-2.7-1.5, has decreased about 74% on average compared to LCF-0.55-0.3 and LCF-0.8-0.45 models. It means that, by increasing the length of the link beam, the LCF system performance is decreased and the shear force is brought into the main frame and the plastic hinges are first formed in the main frame (RC).
- For the model of LCF-0.8-0.45 compared with the two models of LCF-0.55-0.3 and LCF-1.1-0.6, the ratio of the displacement of the structure with the formation of the plastic hinges in the members in the collapse prevention ($\Delta_{p\ LCF}$) to the displacement of the structure with the formation the first plastic hinge in the link beam ($\Delta_{y\ LCF}$) is increased about 14% and 22%, respectively. It means that, the distance between $\Delta_{y\ LCF}$ and $\Delta_{p\ LCF}$ has been increased in the model of LCF-0.8-0.45 and it has more potential to reach the performance level of the RR to occupancy performance level.

Therefore, the best performance of the LCF system and on the models is studied, the model with a ratio of the link beam length (e) to the span length of the RC frame (L) is equal to 0.45 (LCF-0.8-0.45). In this model the plastic hinges are first formed in the link beam of LC fame and the main frame (RC frame) remains elastic phase.

REFERENCES

ABAQUS 6.14. (2016). Analysis users's guide: Volume IV: Elements.

Abdollahzadeh, G. and Banihashemi, M. (2013). "Response modification factor of dual moment-resistant frame with buckling restrained brace (BRB)", *Steel and Composite Structures,* 14(6), 621-636.

ACI Committee 318 (2014). *Building code*

requirements for structural concrete and commentary (ACI 318 R-14), American Concrete Institute: Farmington Hills, MI, USA.

ANSI/AISC 341. (2010). *Seismic provisions for structural steel buildings*, American Institute of Steel Construction, Inc., Chicago, Illinois, USA

Applied Technology Council, (1996). *Seismic evaluation and retrofit of concrete buildings*, ATC-40 report, Redwood City, California.

Bai, J. and Ou, J. (2016), "Earthquake-resistant design of buckling-restrained braced RC moment frames using performance-based plastic design method", *Engineering Structures*, 107, 66-79.

Bouwkamp, J., Vetr, M.G. and Ghamari, A. (2016), "An analytical model for inelastic cyclic response of eccentrically braced frame with vertical shear link (V-EBF)", *Case Studies in Structural Engineering*, 6, 31-44.

Broujerdian, V., Shayanfar, M. and Ghamari, A. (2017), "Corner crack effect on the seismic behavior of steel plate shear wall system", *Civil Engineering Infrastructures Journal*, 50(2), 311-332.

Building Seismic Safety Council. (2000). *Pre-standard and commentary for the seismic rehabilitation of buildings*, Report FEMA-356, Federal Emergency Management Agency, Washington, D.C.

Bypour, M., Gholhakia, M., Kioumarsib, M. and Kioumarsia, B. (2019), "Nonlinear analysis to investigate effect of connection type on behavior of steel plate shear wall in RC frame", *Engineering Structures*, 179, 611-624.

Choi, I.R. and Park, H.G. (2008). "Cyclic test for framed steel plate walls with various infill plate details", *The 14th World Conference on Earthquake Engineering*, October 12-17, Beijing, China.

Choi, I.R. and Park, H.G. (2011). "Cyclic loading test for reinforced concrete frame with thin steel infill plate", *Journal of Structural Engineering*, 137(6), 654-664.

Dargush, G.F. and Soong, T.T. (1995). "Behavior of metallic plate dampers in seismic passive energy dissipation systems", *Earthquake Spectra*, 11(4), 545-568.

Dusicka, P. and Iwai, R. (2007). "Development of linked column frame system for seismic lateral loads", In: *Structural Engineering Research Frontiers*, Long Beach, California, United States, 1-13.

Dusicka, P. and Lewis, G. (2010). "Investigation of replaceable sacrificial steel links", *Proceedings of the 9th U.S. National and 10th Canadian Conference on Earthquake Engineering*, No. 1659. EERI, Toronto, Ontario, Canada.

Fintel, M. and Ghosh, S.K. (1981). "The structural Fuse: An inelastic approach to earthquake-resistant design of buildings", *Civil Engineering*, ASCE, 51(1), 48-51.

Haji, M., Naderpour, H. and Kheyroddin, A. (2019), "Experimental study on influence of proposed FRP-strengthening techniques on RC circular short columns considering different types of damage index", *Composite Structures*, 209, 112-128.

Hemmati, A., Kheyroddin, A. and Farzad, M. (2020), "Experimental study of reinforced concrete frame rehabilitated by concentric and eccentric bracing", *Journal of Rehabilitation in Civil Engineering*, 8(1), 97-108.

Kasai, K. and Popov, E.P. (1984). "On seismic design of eccentrically braced steel frames", *Proceedings of the 8th World Conference on Earthquake Engineering*, San Francisco, CA, July 21-28, 5, 387-394.

Kheyroddin, A., Gholhaki, M. and Pachideh, G. (2019), "Seismic evaluation of reinforced concrete moment frames retrofitted with steel braces using IDA and pushover methods in the near-fault field", *Journal of Rehabilitation in Civil Engineering*, 7(1), 159-173.

Kheyroddin, A., Sepahrad, R., Saljoughian, M. and Kafi, M.A. (2019), "Experimental evaluation of RC frames retrofitted by steel jacket, X-brace and X-brace having ductile ring as a structural fuse", *Journal of Building Pathology and Rehabilitation*, 4(1), 11.

Kianmofrad, F., Ghafoori, E., Motavalli, M. and Rahimian, M. (2018). "Analytical solutions for the flexural behavior of metal beams strengthened with prestressed unbonded CFRP plates", *Civil Engineering Infrastructures Journal*, 51(1), 101-118.

Li, S., Jiang, H. and He, L. (2019), "Study of a new type of replaceable coupling beam in reinforced concrete shear wall structures", *The Structural Design of Tall and Special Buildings*, 28(10), e1620.

Lia, Y.W., Lib, G.Q., Jiangc J., Sun F.F. (2018). "Mitigating seismic response of RC moment resisting frames using steel energy-dissipative columns", *Engineering Structures*, 174, 586-600.

Lin, X., Wu, K., Skalomenos, K.A., Lu, L. and Zhao, S. (2019), "Development of a buckling-restrained shear panel damper with demountable steel-concrete composite restrainers", *Soil Dynamics and Earthquake Engineering*, 118, 221-230.

Lu, X., Chen, Y. and Jiang, H. (2018), "Earthquake resilience of reinforced concrete structural walls with replaceable "fuses"", *Journal of Earthquake Engineering*, 22(5), 801-825.

Malakoutian, M., Berman, J.W. and Dusicka, P. (2013). "Seismic response evaluation of the linked

column frame system", *Earthquake Engineering and Structural Dynamics*, 42, 795-814.

Malakoutian, M., Berman, J.W., Dusicka, P. and Lopes, A. (2016). "Quantification of linked column frame seismic performance factors for use in seismic design", *Journal of Earthquake Engineering*, 20, 535-558.

Mohsenzadeh, V. and Wiebe, L. (2018). "Effect of beam-column connection fixity and gravity framing on the seismic collapse risk of special concentrically braced frames", *Soil Dynamics and Earthquake Engineering*, 115, 685-697.

Nader, M., Baker, G., Duxbury, J. and Maroney, B. (2000), "Seismic design for the self-anchored suspension bridge, san Francisco Oakland bay bridge", *Proceedings of the 12th World Conference on Earthquake Engineering*, Auckland, New Zealand.

Pandikkadavath, M.S. and Sahoo, D.R. (2017). "Mitigation of seismic drift response of braced frames using short yielding-core BRBs", *Steel and Composite Structures*, 23(3), 285-302.

Shahrooz, B.M., Fortney, P.J. and Harries, K.A. (2017), "Steel coupling beams with a replaceable fuse", *Journal of Structural Engineering*, 144(2), 04017210.

Shen, Y., Christopoulos, C., Nabil, M. and Tremblay, R. (2011). "Seismic design and performance of steel moment-resisting frames with nonlinear replaceable links", *Journal of Structural Engineering*, 137(10), 1107-1117.

Shoeibi, S., Kafi, M.A. and Gholhaki, M. (2017). "New performance-based seismic design method for structures with structural fuse system", *Engineering Structures*, 132, 745-760.

TahamouliRoudsari, M., Eslamimanesh, M.B., Entezari A.R., Noori, O. and Torkaman, M. (2018). "Experimental assessment of retrofitting RC moment resisting frames with ADAS and TADAS yielding dampers", *Structures*, 14, 75-87.

Zahrai, S.M., Ezoddin, A. (2018). "Cap truss and steel strut to resist progressive collapse in RC frame structures", *Steel and Composite Structures*, 26**(**5), 635-647.